Co internal oxidation and precipitation in Ag studied by Mössbauer spectroscopy

G. L. Zhang

Shanghai Institute of Nuclear Research, Chinese Academy of Sciences, Shanghai 201800, People's Republic of China

J. Verheyden, W. Deweerd, G. E. J. Koops, and H. Pattyn

Institut voor Kern-en Stralingsfysika, Physics Department, K. U. Leuven, Celestijnenlaan 200D, B-3001 Leuven, Belgium

(Received 2 March 1998)

Because of the insolubility of Co in Ag, it will readily start to segregate after its introduction through ion implantation, eventually forming magnetic clusters in a diamagnetic matrix. Taking advantage of the high sensitivity of Mössbauer emission spectroscopy on implanted ^{57}Co probes, we have followed this precipitation process from the initial stages at a very low concentration of 0.05 at. %. At the lowest concentration, essentially all Co is initially present in a substitutional and dimer form. The Co atoms exhibit a strong reactivity, both with other Co and with O atoms, and we observe that the trace amount of oxygen that is still present in commercial Ag foils strongly interacts with the precipitating Co atoms, leading to molecular Co oxide and extended Co ferrite ($Co_xFe_{1-x}O_4$) structures, which we identify through their hyperfine parameters. The oxygen impurity is also involved in the segregating nanoprecipitates, thereby inhibiting them from reaching a fully ripened stage. Even though the oxygen contaminant hinders the clustering process and induces the formation of additional segregated oxide compounds, the magnetic precipitates still reach a large relative spectral intensity of 10% and 20% in the samples with a quite low Co concentration of, respectively, 0.05 and 0.15 at. %. [S0163-1829(98)04030-2]

I. INTRODUCTION

While noble metals do not react with oxygen at elevated temperatures to form stable oxides, the presence of oxygen can strongly influence their properties. This occurs because a small amount of a less noble element present in the noble metal will react with mobile oxygen atoms, diffusing interstitially through the lattice. This phenomenon is known as internal oxidation. Considerable effort has been devoted to the study of the internal oxidation of metals.[1,2] It was found that small oxide precipitates have a profound influence on the mechanical and electrical transport properties of the material[3,4] and that the crystal structure of the precipitates differs from the one expected from phase diagrams.[5] Significant progress in the understanding of the microstructure of the oxides and the kinetics of internal oxidation was made by the work of Wagner.[6]

On the submicroscopic scale, the process of internal oxidation of dilute In, Sb, or Sn impurity atoms in a silver matrix has been studied by time-differential perturbed angular correlation,[4,5,7–9] Mössbauer spectroscopy, and nuclear reaction and/or channeling techniques.[10–14] In those studies, oxygen was introduced from the outside, either by indiffusion from the gas phase at high temperature or by ion implantation. However, not much attention was paid to the effect of oxygen preexisting in the silver itself. Recently, many experimental studies on magnetic nanoparticles have been carried out because of their interesting magnetic properties[15,16] and their corresponding giant magnetoresistance effect.[17,18] The pronounced affinity of transition-metal nanoparticles for oxygen makes it necessary to study their interactions in more detail. The creation of a forced mixture of Co and Ag, with both elements having a vanishing reciprocal solubility at equilibrium, easily results in a system containing magnetic particles (Co) in a nonmagnetic matrix (Ag). Ion implantation, for instance, readily results in Co cluster formation, even at RT, in as far as the Co concentration exceeds approximately 1 at. % (Ref. 19). This combination has raised a strong interest and has served more or less as a prototype granular magnetic system.

The major part of published research work dealing with Co-Ag granular systems focuses on relatively high Co concentrations, with correspondingly larger precipitates. Since many unusual properties have been predicted theoretically for the smallest clusters, for instance the change in magnetic moment per atom[20] as compared to bulk material, we are concentrating our research on the very small clusters. It is very important to get rid of the influence of trace elements and oxygen in the matrix for this kind of study. The extent of this influence can only be observed by a very diluted impurity in the matrix. One also needs to start from a very diluted system for deriving particular aspects of the cluster nucleation, such as the interaction distance between two impurity atoms. In order to work at a very low Co concentration for the present study, Co was introduced into a silver matrix at RT by implanting radioactive ^{57}Co, followed by stable ^{59}Co ions. The oxidation of the Co atoms was a consequence of the presence of oxygen in the silver foil itself. We used Mössbauer spectroscopy to trace the diffusion process and the configuration of the oxygen and Co atoms and to observe the growth of the Co oxides and Co precipitates. The use of Co atoms as probes instead of Sb, Sn, or In, allows us to determine with more accuracy the location of the oxygen atoms surrounding the probe atom, in particular, the tetrahedral and the octahedral interstitial sites, because Co can form a spinel structure with oxygen. For earlier results from a study by nuclear reaction analysis, using the $^{18}O(p,\alpha)^{15}N$
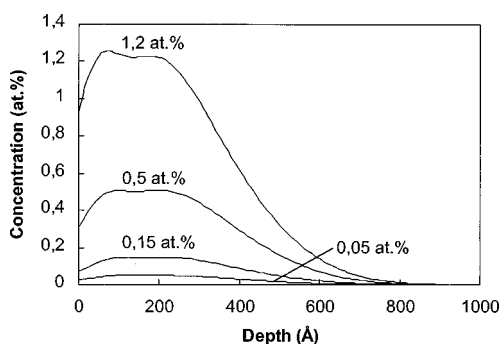
     PRB <u>58</u>   3026

FIG. 1. Implantation profiles of ^{59}Co in Ag, calculated with the TRIM code.

reaction, of the oxygen content in the Sb-O-Ag system as a function of the annealing temperature, we refer to Ref. 14.

II. EXPERIMENT

Four polycrystalline Ag foils (M.R.C., Marz grade, 99.999% total) with a thickness of 120 μm were used as targets. The grain diameter in these Ag foils was determined by optical microscopy and is typically 7.5 μm. In order to study the interaction between impurity atoms and oxygen atoms contained in the Ag foils, the preimplantation with ^{57}Co and postimplantation with ^{59}Co were performed without any pretreatment of the foils. Only the surface was cleaned. The Co concentrations are 0.05, 0.15, 0.5, and 1.2 at. %, respectively. The energies and doses were chosen such that the Co implantation profile was as homogeneous as possible and well overlapping the ^{57}Co depth region. All implantations were done at RT. The implantation parameters can be found in Ref. 19. Figure 1 shows the calculated ^{59}Co implantation profiles.

In addition, two other samples with a Co concentration of 6 at. % were prepared and measured at low temperatures in order to help determine the configurations of the Co-oxygen complexes in Ag. One was pretreated in a reduction furnace before the ion implantation, and the other was not.

The samples were subjected to an isochronal annealing treatment of 30 min in a reducing gas flow, consisting of $H_2 + Ar$. The final step was at an annealing temperature $T_a = 800\,°C$. After each step a Mössbauer spectrum was recorded at RT in the usual transmission geometry versus a Na_4 ^{57}Fe(CN)$_6 \times 10$ H_2O absorber. All reported isomer shifts, however, will be referred to α-Fe at RT.

A particularly attractive aspect of this sample preparation approach is that (a) it is possible to obtain a very low Co concentration in Ag by using radioactive Co atoms as both a probe and impurity, and (b) the oxygen atoms are provided by the Ag matrix itself, mostly from the nonimplanted region.

III. EXPERIMENTAL RESULTS

In Fig. 2 we show a few typical Mössbauer spectra from the sample with 0.05 at. % Co as a function of increasing annealing temperature. It indicates the evolution of the oxidation and precipitation of the Co atoms. The spectra were fitted by a least-squares-fitting routine in a consistent way in which parameters were allowed to vary only between narrow

limits. Six major components were necessary to fit the spectra: a single line, three quadrupole doublets, and two magnetically split multiplets. They are denoted as $S1$, $Q1$, $Q2$, $Q3$, $M1$, and $M2$, respectively. The Mössbauer parameters of four of them are summarized in Table I. The general trends in the behavior of the relative intensity of these components as a function of the annealing temperature are similar for the four lower Co concentrations. The relative intensity of some components is, however, strongly correlated to the Co concentration. This is illustrated in Figs. 3(a) and 3(b), where we plot the intensities for the samples $Co_{0.05}Ag_{99.95}$ and $Co_{0.15}Ag_{99.85}$ as a function of the annealing temperature. In the next two sections, we discuss and identify the nature of these components.

A. Isochronal annealing behavior of the components for the four samples with Co concentrations $\leqslant 1.2$ at. %

Component $S1$. The single line clearly originates from substitutional ^{57}Fe in the Ag matrix. Its isomer shift (IS) is 0.48(2) mm s^{-1} on average, in accordance with the value measured earlier by Sawicka[21] and our group.[19] Its relative intensity in the as-implanted samples decreases markedly, from 65% to 16%, when the Co dose increases from 0.05 to 0.15 at. %, and then fluctuates with a further increase in dose. In Fig. 3(a) we show that in the 0.05 at. % sample its intensity decreases from 65% to 4% with annealing temperature from RT to 600 °C, after which it increases again with annealing temperature to 60% at $T_a = 800$ °C. In the sample with the next higher concentration, as shown in Fig. 3(b), its intensity is already much lower at the onset, in favor of component $Q1$. The general trend is, however, quite similar.

Component $Q1$. This component is represented by a quadrupole split doublet with the following parameters: IS$=0.34-0.45$ mm s^{-1} and splitting $\Delta_{QS}=0.64-0.68$ mm s^{-1}. We assigned it to the contribution from ^{57}Fe-Co dimers. We have already discussed the spectra from the as-implanted samples in Ref. 19, where we fitted them as a function of the Co concentration. It is understandable that some parameters are slightly different here, as we now made a consistent fit as a function of the annealing temperature. This component reaches the highest intensity (70%) for the as-implanted sample with 0.15 at. % Co. The variation of the intensity with the annealing temperature is not smooth. It strongly depends on oxygen migration and trapping at Co atoms. It will be discussed later on.

Component $Q2$. This component shows a large isomer shift and quadrupole splitting: IS$=1.00-1.20$ mm s^{-1} and $\Delta_{QS}=2.06-2.40$ mm s^{-1}. These values are typical for Fe^{2+} ions in the high-spin state, which was also formed in MgO by classical doping and ion implantation.[22,23] The contribution of the Fe^{2+} component in the spectra increases with T_a up to 400 °C and decreases afterwards. The maximal relative intensity decreases with the Co concentration (see Fig. 4). A surprisingly high fraction of 60% of the Co atoms is found to be oxidized by the internal oxygen for sample $Co_{0.05}Ag_{99.95}$.

Component $Q3$. This component only becomes apparent in the Mössbauer spectra at the higher annealing temperatures, starting from 500 °C. It is formed out of the dimer ($Q1$) and $Q2$. The isomer shift and quadrupole splitting are 0.80–0.90 mm s^{-1} and 0.5–0.8 mm s^{-1}, respectively. These values are close to the parameters of $Fe_{0.9}O$ (Ref. 24) and FeO (Ref. 25). The Fe ions are located in complexes with a
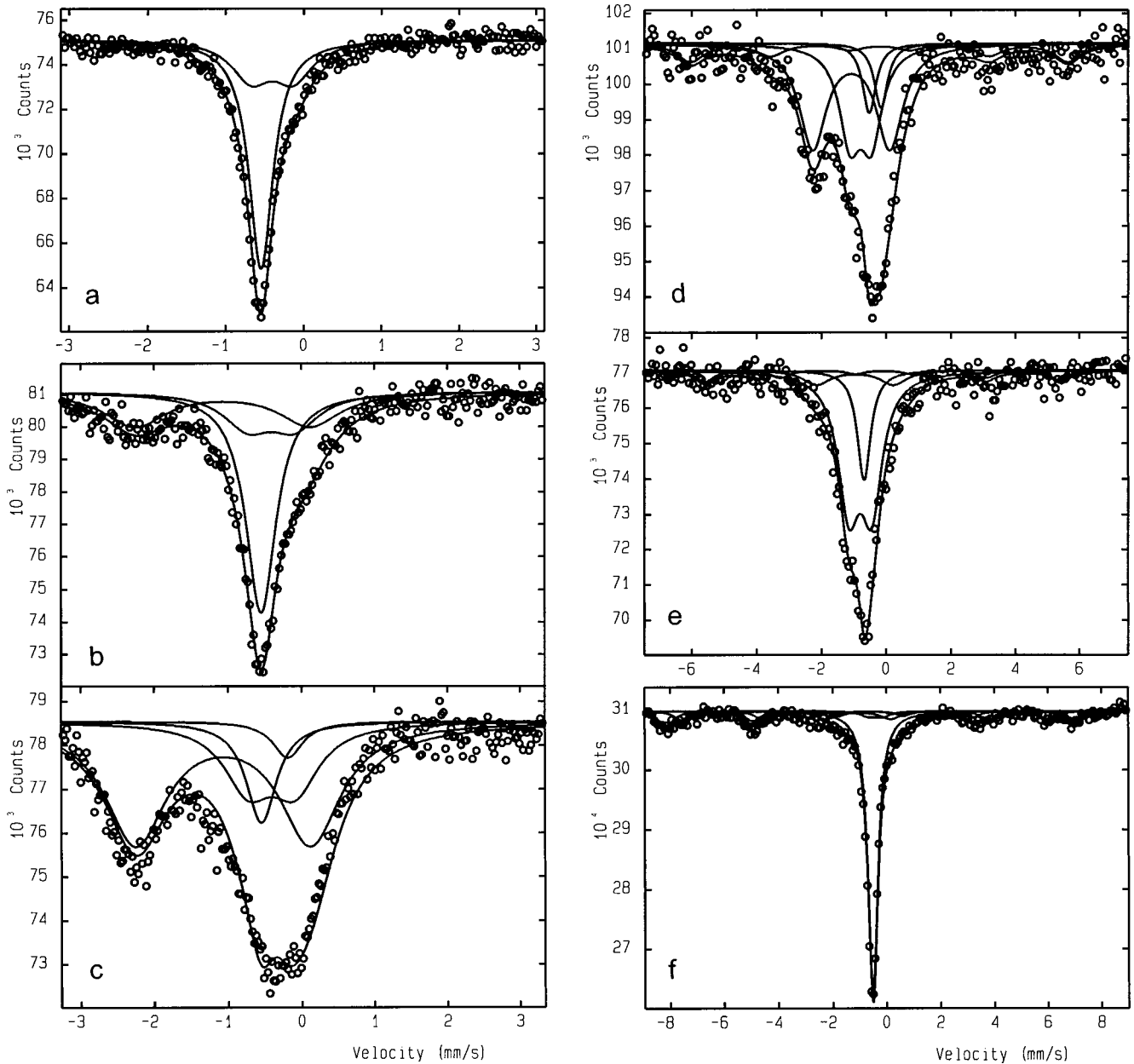
FIG. 2. RT Mössbauer spectra and least-squares fits from $Co_{0.05}Ag_{99.95}$ annealed at (a) RT, (b) 150, (c) 400, (d) 500, (e) 700, and (f) 800 °C.

higher symmetry than those corresponding to $Q2$. We will discuss the configuration more in detail later on. After annealing at 800 °C, this complex has dissociated completely in favor of the substitutional fraction and of the ferrite component (cf. further, $M2$) for the sample with the lowest Co

TABLE I. Mössbauer parameters of the Co complexes in Ag.

Complex label	IS (mm s^{-1})	Δ_{QS} (mm s^{-1})	H (T)
$S1$	0.48(2)		
$Q1$	0.34–0.45	0.64–0.68	
$Q2$	1.0–1.2	2.06–2.40	
$Q3$	0.8–0.9	0.5–0.8	
$M1$	0.06		33.7

concentration, and it remains to some extent for the other samples, as is shown in Fig. 5.

Component M1. This component appears as a sextuplet in the spectra. We ascribe it to precipitates with ferromagnetic properties above RT. It has an isomer shift of 0.06 mm s^{-1} and a mean magnetic hyperfine field of 33.7 T. The isomer shift is close to the value of 0.04 mm s^{-1} (Ref. 26) but the field is about 8% larger than the values for fcc-Co (Ref. 27) and hcp-Co (Ref. 28). We believe that this increase results from the chemisorption of oxygen in the particles and the incorporation of Fe atoms. We will discuss this further on. In all samples $M1$ appears around $T_a = 350$ °C, except for the lowest concentration, where it is preceded by the component $S2$. This precipitation process takes place through the intermediary of the Co dimers ($Q2$) as we will discuss later. Annealing at 800 °C makes it disappear from all samples.
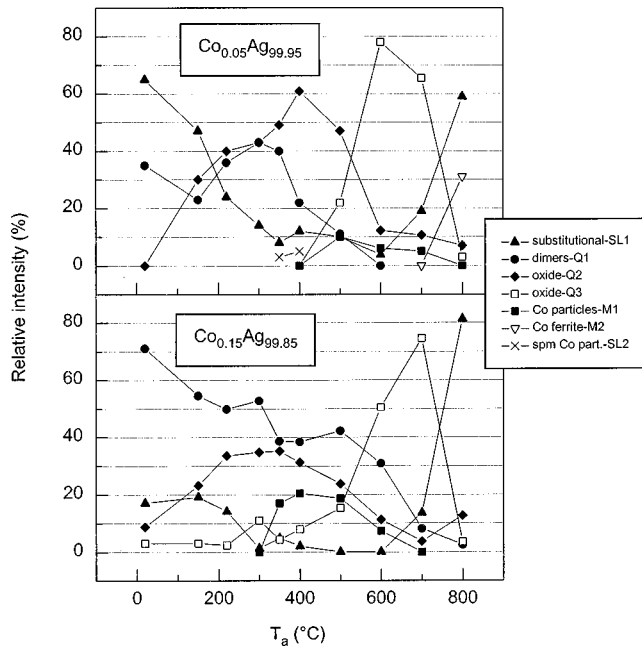
FIG. 3. Relative intensities of the components in the Mössbauer spectra at RT taken as a function of annealing temperature from (a) sample $Co_{0.05}Ag_{99.95}$ and (b) sample $Co_{0.15}Ag_{99.85}$.

The dependence of the maximal relative intensity on the Co concentration is shown in Fig. 4. We see that, even for the very low Co concentration of 0.05 at. %, its maximum intensity already reaches 10%. The annealing temperature at which the maximum intensity is reached is between 400 and 500 °C for the four samples. It means that Co particle growth is most effective in this temperature region. A typical spectrum is shown in Fig. 5 for the sample with 0.5 at. % Co. The fact that the intensity does not increase very much with the Co concentration from 0.15 to 1.2 at. % is an indication of growth inhibition that we ascribe to an oxidation effect, as will be discussed later on.

Component S2. The magnetic clusters have a certain size distribution. At the lowest Co concentration and a lower annealing temperature, where a correspondingly smaller mean size is expected, part of them may still have their blocking temperature below RT. They will exhibit a superparamagnetic behavior at this measuring temperature and appear as a broadened single line with an isomer shift close to that of component $M1$. We do indeed observe such a component in
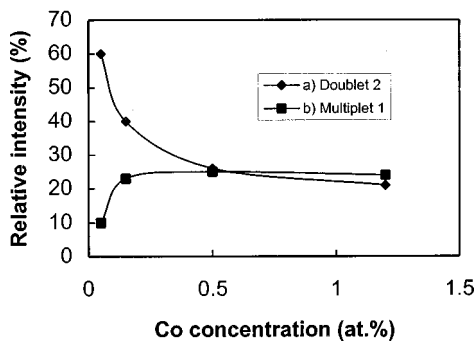

FIG. 4. (a) Maximum relative spectral intensity vs the Co concentration of (a) doublet 2 ($Q2$) and (b) multiplet 1 ($M1$).
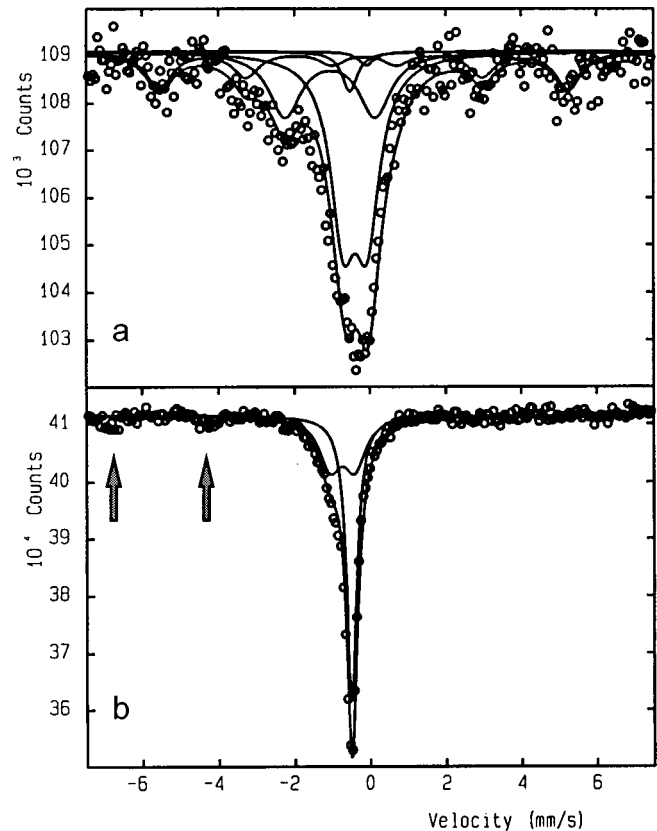

FIG. 5. RT Mössbauer spectra and least-squares fits from $Co_{0.5}Ag_{99.5}$ annealed at (a) 500 and (b) 800 °C. The Co ferrite component is indicated by the two arrows in (b).

the temperature interval 350–400 °C, which is identified as single line $S2$ in Fig. 3(a). This component shows up just before the size distribution of the clusters shifts to larger values and appears as $M1$.

Component M2. This component corresponds to a spinel structure compound. As usual, we call the Co_A (surrounded by 4 O atoms) and Co_B atoms (surrounded by 6 O atoms) in the compound the tetrahedral and the octahedral site, respectively. This component consists of two magnetic fields, field A (about 47 T) and field B (about 43 T). $M2$ only appears clearly in the spectra of $Co_{0.05}Ag_{99.95}$ after annealing at 800 °C. Its intensity decreases rapidly with increasing Co concentration. We could only see a weak indication of this component for Co concentrations up to 0.5 at. %, as indicated in Fig. 5. The reason is that, for the higher Co concentrations, the Ag foil has a limited oxygen supply for the combination with the Co atoms to form this compound.

Polycrystalline spinel compounds are usually synthesized by solid-state reactions, starting from an intimate mixture of oxides with the appropriate ratio of metal ions. Commonly, it is formed after heating at 1000 °C. However, in the present case of ion implantation, this compound can already be formed at 800 °C.

B. Characterization of the oxide of component $Q3$ at low temperatures

As mentioned before, above 400 °C the component $Q3$ appears in the spectra, as can be seen in Figs. 2(d), 2(e), and 5(a). It seems to be an intermediate state in the transition
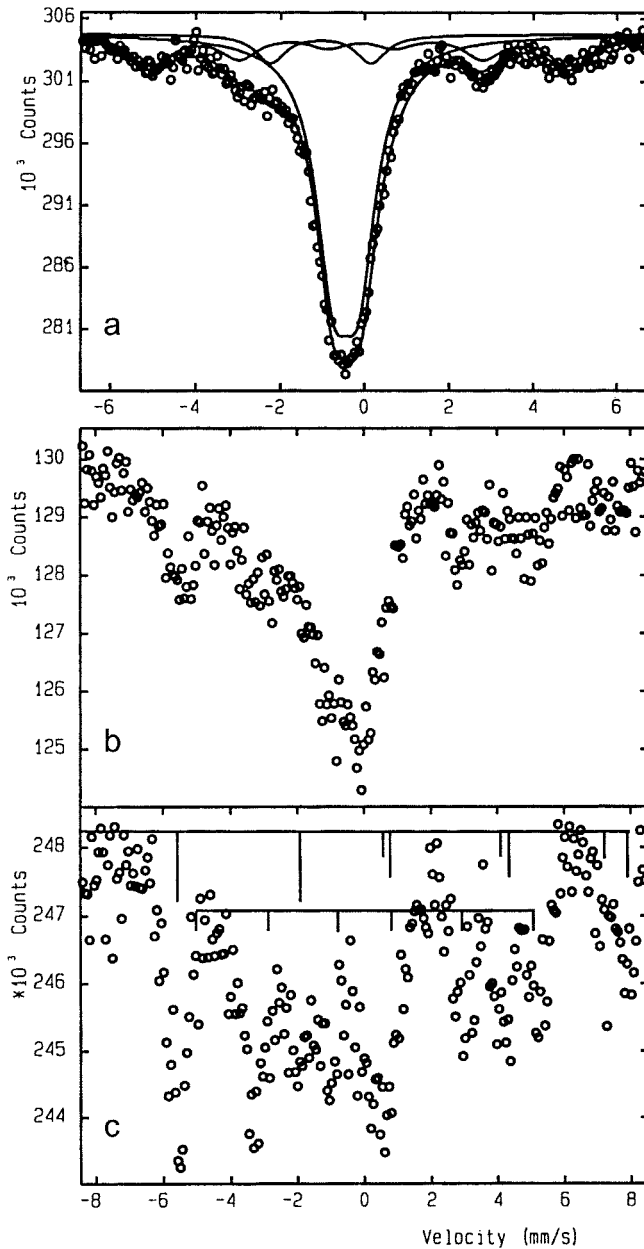
FIG. 6. Mössbauer spectra from Co_6Ag_{94} annealed at 510 °C, measured at (a) RT, (b) 90 K, and (c) 10 K.

from $Q2$ to $M2$. In order to clarify this component, we made a sample with 6 at. % Co in the same conditions as the other four samples. The reason for choosing such a high concentration is that we observed that the maximal intensity of $Q3$ is larger for higher Co concentrations, where little or no Co ferrite ($M2$) is formed and where, furthermore, the intensity of the precipitate component ($M1$) saturates with increasing Co concentration. The sample was measured after an annealing step at 510 °C. Three spectra, recorded at 10, 90, and 293 K, are presented in Fig. 6. The spectrum in Fig. 6(a) can only be deconvoluted in one sextuplet and two doublets. The sextuplet has an isomer shift of 0.04 mm s^{-1} and a hyperfine field of 31.2(1) T. One doublet corresponds to $Q2$ and has a low intensity. The other doublet with dominant intensity is located at the center of the spectrum and has new values for the isomer shift and quadrupole splitting. Both the sextuplet and the latter doublet have a linewidth larger than 1 mm s^{-1}.
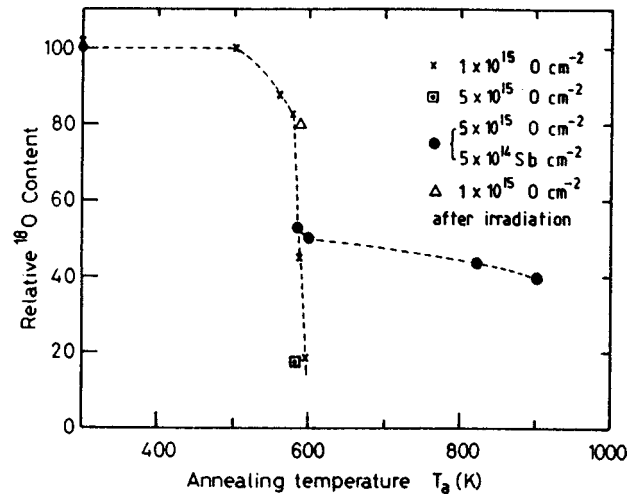

FIG. 7. Relative O content as a function of annealing temperature for three Ag crystals implanted with different O and Sb doses as indicated (Ref. 14).

Both these components could be further deconvoluted after collecting a spectrum at 90 K. The magnetically split part consists of two hyperfine fields. Their isomer shifts and fields are 0.04(3) and 0.11(3) mm s^{-1} and 34.5(3) and 31.4(5) T, respectively. The broad central doublet could be further deconvoluted in one single line originating from small superparamagnetic particles and a quadrupole split doublet with the same parameters as $Q3$. At 10 K, $Q3$ is seen to change partly into two magnetic multiplets with fields larger than 51 T, as can be seen in Fig. 6(c). The one with the highest field has a larger intensity. It means that $Q3$ might be ascribed to nonstoichiometric magnetite.

In addition, we measured a sample with 6 at. % Co implanted in an Ag foil annealed in H_2 at 800 °C before the Co implantation, in order to compare it with the sample without pretreatment. The spectra show that no component corresponding to the oxides is present at any annealing step, and that the fraction of Co precipitates ($M1$) is much higher.

IV. DISCUSSION

A. Introduction on the behavior of oxygen after implantation of O and Sb in Ag

Before we discuss the experiments described here, we will first resume the oxygen behavior in Ag as it was observed some years ago,[14] in order to understand the Co oxidation process during annealing and the oxygen effect, even in samples that were annealed in a mixture of H_2 and Ar.

Figure 7 shows the relative oxygen content as a function of annealing temperature for three Ag crystals implanted with different O and Sb doses as taken from Ref. 14. The O concentration was determined by measuring the ^{18}O depth profile using the $^{18}O(p,\alpha)^{15}N$ reaction. It was found that the O atoms had diffused during the RT implantation. A fraction of 49% (at 583 K) to 40% (at 900 K) of the initial oxygen amount present in the implanted and damaged region is retained in the sample coimplanted with ^{18}O and ^{121}Sb. Apparently, in this sample smaller fractions escape from this region after implantation and after annealing, compared to the fractions observed in the sample implanted with ^{18}O

only. From this experiment we learned that the migration temperature of O depends strongly on the defects O is associated with, such as vacancies and impurity atoms. In view of these results, we can understand what happened in the present case by taking into account that the activation energies and the electronegativities of Co and Sb atoms are essentially the same.[29,30]

B. O migration and association with impurity atoms in the regime $T_a < 400\,°C$

We will first discuss the regime below $T_a = 400\,°C$, in which the relative intensity of the Co oxide component $Q2$ increases strongly with the annealing temperature. The commercial Ag foils contain a certain amount of dissolved oxygen in the form of free interstitial oxygen atoms or of Ag_2O molecules. The former ones, with their low migration energy of only 0.48 eV,[31] migrate already at RT; the Ag_2O compound dissociates around 150 °C.[31] The implantation process has probably induced the formation of oxygen-vacancy complexes as well, which would make the oxygen reservoir consist of three forms. The interactions that take place in the present temperature interval are most clearly observed in the lowest concentration sample, as shown in Fig. 3(a).

Based on the Co diffusion coefficient in Ag,[29] we may not expect that substitutional Co atoms ($S1$) become mobile before 300 °C. Nonetheless, the first annealing step at 150 °C already decreases its relative population, and this process is further accelerated by the next step at 200 °C. It is plausible that the excess vacancies left from the implantation process are responsible for a certain increase in the low range mobility of the Co atoms. The radiation enhanced migration process is thought to have been in action already during the implantation, causing an acceleration of the primary nucleation, corresponding to a speedup of the transition from substitutional sites ($S1$) to dimer sites ($Q1$). Right after the implantation, we indeed find a relative population of the dimer component that exceeds, by far, the statistically expected value: it reaches 35% at 0.05 at. % and already 72% at 0.12 at. %, pointing to a rather large interaction radius (cf. also Ref. 19). While an enhanced Co mobility can explain the abrupt decrease of the $S1$ intensity in the lowest concentration sample, this may also partly be due to oxygen trapping. This hypothesis would require that component $Q2$ encompasses as well the association of oxygen with single Co(Fe) atoms, as with Co(Fe)-Co pairs. A linear structure might be the reason for the limited sensitivity of the hyperfine parameters to the presence of a second Co atom in such a structure.

The trapping of oxygen at the dimers ($Q1$) is already so prominent, even at $T_a = 150\,°C$, that the feeding of the dimers from substitutional Co in the lowest concentration case is overcompensated by a further feeding of the $Q2$ site from the dimers. The acceleration in the dimer formation in the next two annealing steps, at $T_a = 200$ and 300 °C, allows for a temporary increase in its relative population. Later on, at higher annealing temperatures, up to $T_a = 400\,°C$, the growth curve is finally overtaken by the continued transition towards $Q2$, the oxygen associated component. This steep

rise in the relative $Q2$ population is probably also a consequence of the mobility of oxygen-vacancy complexes, which starts around 300 °C.[7,14,22,32]

Based on the hyperfine parameters of $Q2$, we can assign it to Fe^{2+} ions in the high-spin state, located at low-symmetry sites. Since it appears already around 150 °C, even in the sample with the lowest Co concentration, we believe that it must correspond to a rather simple Co oxide molecule, involving a maximum of two Co atoms. We exclude larger entities since we have not yet observed precipitated clusters. The geometrical arrangement of the $Q2$ complex remains unknown. Any thorough discussion on this point needs to start from an investigation of the dimer configuration (in preparation). Based on the high quadrupole splitting, caused by a high asymmetry, we can suggest that it probably contains one O atom and possibly one or more vacancies. A similar defect has been identified containing In, oxygen and vacancies, which could survive in Ag up to high annealing temperatures.[7] In the present case we find that this complex still exists above 500 °C. Based on the large linewidth of 1 mm s^{-1} of this component, as shown in Fig. 2, decreasing slightly with annealing temperature, we believe that this compound does not correspond to a unique structure. We assign it tentatively to $Co_2O_mV_n$ or CoO_mV_n where V stands for a vacancy.[14]

C. Co oxide forming Co ferrite in the regime $T_a = 400–800\,°C$

As can be seen in Fig. 3, the intensity of the oxide component $Q2$ starts to decrease from $T_a = 400\,°C$, along with that of the dimers. The intensity of those components is taken up by another Co oxide component ($Q3$), finally forming Co ferrite at 800 °C. In this temperature regime, even though it is hard to understand all the details, several important processes could take place: (1) the diffusivity of single Co atoms becomes important at $T_a > 350\,°C$; (2) at $T_a > 350\,°C$ thermally created vacancies start playing their role; (3) part of the smaller O_mV_n complexes that could have formed by the diffusion of oxygen into the implanted zone will dissociate (see Fig. 7). As mentioned above, some part of the Co oxide ($Q3$) appears as a magnetic sextuplet in the Mössbauer spectrum at 10 K and as a superparamagnetic doublet above 90 K, implying that these particles have a size of about 2 nm.[33] Figures 3(a) and 3(b) show that around $T_a = 600–700\,°C$ almost 80% of the Co atoms are present in the Co oxide form corresponding to $Q3$, and that at 800 °C this component essentially transforms into substitutional Co ($S1$), although in the lowest concentration sample, $Co_{0.05}Ag_{99.95}$ [Fig. 3(a)], 30% is transformed into a Co ferrite form. The magnitude of this fraction implies that the Co oxide molecules ($Q2$) become mobile at $T_a > 400\,°C$: if each $Q2$ molecule was a precipitation center, the total amount of implanted Co atoms would not be sufficient to provide for the formation of so many particles. Therefore, we conclude that, at $T_a > 400\,°C$, the Co oxide clusters ($Q3$) form from a coagulation of the Co oxide molecules ($Q2$) combined with the remaining dimers ($Q1$).

As mentioned in Sec. III, the Mössbauer parameters of $Q3$ (IS = 0.8–0.9 mm s^{-1}, $\Delta_{QS} = 0.5–0.8$ mm s^{-1}) are close to the wüstite $Fe_{0.9}O$ compound with the NaCl structure. Co oxide has the same structure as Fe oxide above 291 K.[34] We

also found that part of the $Q3$ intensity turns into a magnetically split component at 10 K. Furthermore, this component is present up to 800 °C and the retained intensity increases with the Co concentration. Based on these observations, we suspect that $Q3$ consists of at least two components. One component arises from small particles of Co ferrite, which eventually form larger particles during further annealing. The other component arises from the Co wüstite phase, which can turn into Co ferrite if there is a sufficient supply of oxygen. This transition process was equally found in the case of MgO implanted with Fe.[23,35] In Sec. IV D, we argue that both the Co ferrite and Co wüstite phase contain Fe atoms as well.

D. Co precipitates in Ag

1. Component M1

$M1$ corresponds to ferromagnetic Co particles in Ag and starts to form at $T_a = 450$ °C for the sample with 0.05 at. % Co. Under different conditions, Co metal can take, alternatively, the fcc, bcc, or hcp structure. In the present case, the structure of Co particles in Ag is hard to establish by x-ray diffraction, even in the glancing angle mode due to the very low amount of Co. We find that the observed hyperfine field of 33.7 T is higher than the value for pure Co, which is 31.2 T for fcc Co (Ref. 27) and 31.6 T for hcp Co (Ref. 28). This effect, as mentioned in Sec. III, may be caused by chemisorption of oxygen at interface atoms, because strongly bound O containing iron compounds have a higher field value.[36] In the temperature range $T_a > 400$ °C, as discussed before, the oxygen-vacancy complex dissociates and the Co oxide molecule becomes mobile, allowing O atoms to get trapped during the formation of the Co precipitates. Two observations support this: (1) we measured a value around 27–29 T for clean interfaces in annealed samples;[37] (2) for the sample with 6 at. % Co, where the ratio of O to Co is much smaller and the effect of oxygen on the field in the particles is insignificant, we measured the mean value of 31.2 T. A second factor that may contribute to the increase of the magnetic hyperfine field is the incorporation in the magnetic clusters of Fe atoms,[38,39] which are present as an impurity in the Ag foil. We believe that both contaminants contribute. Indeed, the presence of oxygen is revealed in another way, as discussed hereafter, while, if Fe was contributing alone, it would need to represent around 40% of the magnetic cluster.[39]

The particle growth is much more influenced by the absorbed oxygen than the hyperfine field, because the observed maximal fraction of the Co precipitates for the 6 at. % samples is much smaller in the sample without pretreatment. It seems that one monolayer of oxygen or even less at the particle's interface already inhibits the ripening process of precipitates.

We can estimate the size of the particles from the equation for the superparamagnetic relaxation time.[40] For a blocking temperature of the Co particles above RT and an observation time for ^{57}Co$\rightarrow^{57}$Fe Mössbauer spectroscopy of 10^{-8} s, we estimate the minimum particle radius to be 17 Å if the anisotropy constant has the bulk value [4.5×10^5 J m^{-3} (Ref. 41)]. If chemisorption of atoms like O takes place,[42] the anisotropy constant can be considerably higher. If it would be $5 \ 10^6$ J m^{-3}, the particle radius would

be 8 Å. From the Mössbauer results of the sample with 6 at. % Co annealed at $T_a = 510$ °C, we could deduce a mean particle radius of 3.5 nm from the ratio of the relative intensities of interface to interior atoms, a value that is comparable to these estimated values.

The intensity changes in the 300–400 °C temperature range, as plotted in Fig. 3(a), hint to the role played by the dimer fraction ($Q1$) in the process of $M1$ segregation, while the (low) substitutional fraction seems not to be the main player involved. At the slightly larger concentration, displayed in Fig. 3(b), the substitutional Co atoms are clearly completely absent. The implications of this observation on the stability or mobility of the dimer component are not yet clear.

Finally, we like to point out that the precipitation already takes place for a Co concentration as low as 0.05 at. %. This implies that the interaction between the Co atoms must be strong and long ranged, since the Co would otherwise diffuse out of the implanted zone and be lost, once they become mobile, precisely as happens at 800 °C. From the observed change in relative intensity of the substitutional fraction after the implantation, we estimated an interaction radius of 32 Å.[19]

2. Component M2

Co_3O_4 has the normal spinel structure $Co^{2+}(Co_2^{3+})O_4$.[43,44] The Co^{2+} atom on the A site orders antiferromagnetically at 40 K and the Co^{3+} ($3d^6$) atoms on the B site are diamagnetic. In our case, we still observe two magnetically split components at RT. Therefore, $M2$ cannot be assigned to Co_3O_4. The $5N$ Ag foil that we employed here contains Fe (2 ppm) and Cu (0.7 ppm) as some of the major impurities. This corresponds, for a sample thickness of 120 μm, to a total amount of about 10^{15} at. cm^{-2}, several times larger than the amount of implanted Co for sample $Co_{0.05}Ag_{99.95}$ (see Ref. 19). Moreover, an extra Fe dose was coimplanted during the ^{57}Co implantation, which was relatively important for this lowest concentration sample. The Fe atoms behave very similarly to Co and become mobile above 300 °C. It thus seems plausible that Fe-Co-O complexes form from Fe atoms that migrate and get trapped by Co-O complexes. Because of its magnetic hyperfine fields and their relative intensities, we suggest that this complex corresponds to a, probably nonstoichiometrical, Co ferrite like $Co_xFe_{3-x}O_4$.[45] This discussion applies equally to $Q3$, as this may be wüstite $Co_xFe_{1-x}O$.

V. CONCLUSIONS

The formation of various Co-O complexes and Co precipitates after implantation of Co in Ag has been studied by means of Mössbauer spectroscopy. Co oxide molecules are formed above RT by Co dimers, and may be atoms binding to oxygen that preexists in the Ag foil. These are not formed in an Ag foil that was pretreated by annealing at 800 °C in a $H_2 + Ar$ mixture. The fraction of these molecules increases up to $T_a = 400$ °C at the expense of the Co dimers, and possibly of substitutional Co. Then they become mobile and finally form Co ferrite at $T_a = 800$ °C via an intermediate Co-O complex, in particular in the sample with the lowest Co concentration (0.05 at. %). Co ferrite is found in an Ag matrix

with incoherent growth. Fe impurities are probably also involved in the Co ferrite. Meanwhile, Co precipitation takes place between 350 and 450 °C for Co concentrations between 0.05 and 1.2 at. %. The maximum fraction of the precipitates increases with Co concentration. The trapping of oxygen influences the magnetic hyperfine fields of the precipitates and cluster growth will always be partly suppressed if the Ag matrix is not free from oxygen. Therefore, in order to avoid the observed oxygen effects, one should be careful in the preparation of systems of a diluted magnetic element in a noble metal.

In addition, these experiments show that Mössbauer source experiments with ^{57}Co(Fe) are very effective in studying internal oxidation and detecting the presence of trace concentrations of oxygen. Our results indicate that the presence of ppm amounts of oxygen in Ag can be revealed. We are initiating the investigation of the structures of the various Co-O complexes.

[1] R. A. Rapp, Corrosion **21**, 382 (1965).

[2] F. R. Ficket, Mater. Sci. Eng. **14**, 199 (1974); J. Phys. F **12**, 1753 (1982).

[3] A. C. Ehrlich, J. Mater. Sci. **9**, 1064 (1974).

[4] J. Desimoni, A. G. Bibiloni, L. Medoza-Zelis, A. F. Pasquevich, F. H. Sanchez, and A. López-García, Phys. Rev. B **28**, 5739 (1983).

[5] P. Wodniecki and B. Wodniecka, Hyperfine Interact. **12**, 95 (1982).

[6] C. Wagner, Z. Elektrochem. **63**, 772 (1959).

[7] W. Bolse, P. Wodniecki, H. Schröder, M. Uhrmacher, and K. P. Lieb, Phys. Lett. **93A**, 429 (1983).

[8] H. Schröder, W. Bolse, M. Uhrmacher, P. Wodniecki, and K. P. Lieb, Z. Phys. B **65**, 193 (1986), and references therein.

[9] W. Segeth, Ph.D. thesis, University of Groningen, 1987.

[10] G. P. Huffiman and H. H. Podgurski, Acta Metall. **21**, 449 (1973).

[11] F. H. Sanchez, R. C. Mercader, A. F. Pasquevich, A. G. Bibiloni, and A. López-García, Hyperfine Interact. **20**, 295 (1985).

[12] W. Segeth, H. Andreasen, D. O. Boerma, and L. Niesen, Nucl. Instrum. Methods Phys. Res. B **15**, 625 (1986).

[13] H. Andreasen, Ph.D. thesis, University of Groningen, 1987.

[14] G. L. Zhang, H. Andreasen, D. O. Boerma, L. Niesen, and W. Segeth, Phys. Rev. B **39**, 1068 (1989).

[15] G. L. Zhang and Shijun Yu, Phys. Lett. A **222**, 203 (1996).

[16] G. L. Zhang and Shijun Yu, J. Phys.: Condens. Matter **9**, 1851 (1997).

[17] A. Milner, A. Gerber, B. Groisman, M. Karpovsky, and A. Gladkikh, Phys. Rev. Lett. **76**, 475 (1996).

[18] J. Q. Xiao, J. S. Jiang, and C. L. Chien, Phys. Rev. Lett. **68**, 3749 (1992).

[19] J. Verheyden, G. L. Zhang, J. Dekoster, A. Vantomme, W. Deweerd, K. Milants, T. Barancira, and H. Pattyn, J. Phys. D **29**, 1316 (1996).

[20] F. Liu, M. R. Press, S. N. Khanna, and P. Jena, Phys. Rev. B **39**, 6914 (1989).

[21] B. D. Sawicka, Radiat. Eff. **48**, 25 (1980).

[22] H. Wiedersich, U. Gonser, R. W. Grant, and A. H. Muir, Bull. Am. Phys. Soc. **10**, 709 (1965).

[23] A. Perez, G. Marest, B. D. Sawicka, J. A. Sawicki, and T. Tyliszczak, Phys. Rev. B **28**, 1227 (1983).

[24] D. P. Johnson, Solid State Commun. **7**, 1785 (1969).

[25] R. W. Vaughan and A. J. Drickamer, J. Chem. Phys. **47**, 1530 (1961).

[26] S. M. Qaim, Proc. Phys. Soc. (London) **90**, 1065 (1967).

[27] A. M. Portis and A. C. Gossard, J. Appl. Phys. Supp. **31**, 2055 (1961).

[28] G. J. Perlow, C. E. Johnson, and W. Marshal, Phys. Rev. **140**, A875 (1965).

[29] J. Askill, *Handbook of Chemistry and Physics*, 66th ed (Chemical Rubber, Cleveland, 1985), p. F-46.

[30] P. Lof, Elsevier's periodic table of the elements.

[31] W. Eichenauer and G. Müller, Z. Metallkd. **53**, 321, 700 (1962).

[32] L. Thomé and H. Bernas, Hyperfine Interact. **5**, 361 (1978).

[33] F. Bødker, S. Mørup, and S. Linderoth, Phys. Rev. Lett. **72**, 282 (1994).

[34] G. K. Wertheim and D. N. E. Buchanan, in *The Mössbauer Effect*, edited by D. M. J. Compton and A. H. Schoen (Sacley-Wisley, New York, 1962).

[35] U. Gonser, H. Wiedersich, and R. W. Grant, J. Appl. Phys. **39**, 1004 (1968).

[36] S. Bhagwat, S. N. Yedave, D. M. Phase, S. M. Chaudhari, S. M. Kanetka, and S. B. Ogale, Phys. Rev. B **40**, 700 (1989).

[37] J. Verheyden, S. Bukshpan, J. Dekoster, A. Vantomme, W. Deweerd, K. Milants, T. Barancira, G. L. Zhang, and H. Pattyn, Europhys. Lett. **37**, 25 (1997).

[38] G. S. Collins and B. H. Meeves, Scr. Metall. Mat. **29**, 1319 (1993).

[39] E. Jartych, J. K. Zurawicz, and M. Budzynski, J. Phys.: Condens. Matter **5**, 927 (1993).

[40] L. Néel, Ann. Geophys. (C.N.R.S.) **5**, 99 (1949).

[41] B. D. Cullity, *Introduction to Magnetic Materials* (Addison-Wesley, Reading, MA, 1972).

[42] S. Mørup, Phys. Scr. **25**, 713 (1982).

[43] W. L. Roth, J. Phys. Chem. Solids **25**, 1 (1963).

[44] C. D. Spencer and D. Schroeer, Phys. Rev. B **9**, 3658 (1974).

[45] E. De Grave, R. M. Persoons, R. E. Vandenberghe, and P. M. A. de Bakker, Phys. Rev. B **47**, 5881 (1993); **47**, 5894 (1993).